Structure and Spectroscopic Properties of the Crystalline Structures Containing Meridional and Facial Isomers of Tris(8-hydroxyquinoline) Gallium(III)

Martin Brinkmann,*,† Benjamin Fite,† Sirapat Pratontep,† and Christian Chaumont‡

Institut Charles Sadron, 6 rue Boussingault, 67083 Strasbourg, France, and Ecole de Chimie des Polymères et Matériaux (ECPM), 23 rue du Loess, 67000 Strasbourg, France

Received March 18, 2004. Revised Manuscript Received May 6, 2004

The various polymorphs of tris(8-hydroxyquinoline) gallium(III) (GaQ_3) have been prepared and identified in powders and thin films. Three nonsolvated polymorphs have been identified, and their structures have been obtained from powder X-ray diffraction (PXRD). GaQ_3 polymorphs were found to be isomorphous to the α, β, and δ structures reported for the aluminum analogue tris(8-hydroxyquinoline) aluminum(III) (AlQ_3). The α, β, and the solvated structures are racemates of the meridional isomer, whereas the δ polymorph, formed by annealing the α form to 380 °C under vacuum, contains the facial isomer as demonstrated by FT-IR spectroscopy. The α→δ phase transformation can be described as a thermal isomerization reaction in the solid state that largely preserves the unit cell parameters of the initial α structure. Transmission electron microscopy (TEM) and electron diffraction demonstrate that the α structure is formed in oriented films on poly(tetrafluoroethylene) substrates for a substrate temperature T_s = 100 °C. Evidence is found for a high level of structural defects within needles of α GaQ_3. The fluorescence at 293 K of the crystal structures containing *mer* GaQ_3 exhibits the same structural dependence as observed in the case of AlQ_3: the maximum of fluorescence is red-shifted with increasing density of the crystal structure.

I. Introduction

Metal quinolinates based on 8-hydroxyquinoline are known as key materials in the design of organic light-emitting diodes (OLEDs).[1,2] Tris(8-hydroxyquinoline) aluminum(III) is the most well-known molecule of this family, and is extensively used in multilayer OLEDs.[3] This metal chelate is a stable polar and chiral molecule that can exist in the form of two isomers, meridional (*mer*) with C_1 symmetry and facial (*fac*) with C_{3v} symmetry (see Figure 1). Metal chelates such as the gallium analogue tris(8-hydroxyquinoline) gallium(III) have also been considered in OLED architectures by Burrows and co-workers.[4] It has been reported that OLEDs containing GaQ_3 exhibit higher electroluminescence yields than equivalent devices based on AlQ_3 or InQ_3.[4] Recent work has focused on the polymorphism of AlQ_3 and the impact of the crystal packing on the optical properties such as fluorescence.[5] Three nonsolvated and racemic structures (α, β, and γ) of the meridianal (*mer*) isomer of AlQ_3 as well as various clathrates with solvent molecules such as methanol or C_6H_5Cl have been refined. Crystalline thin films of the α structure have been grown on oriented substrates of poly(tetrafluoroethylene) (PTFE) at a substrate temperature T_s = 100 °C,[6] whereas films consisting of amorphous droplets have been observed on apolar H-passivated Si(100) substrate because of a partial wetting.[7] More recently, Brütting and co-workers man-

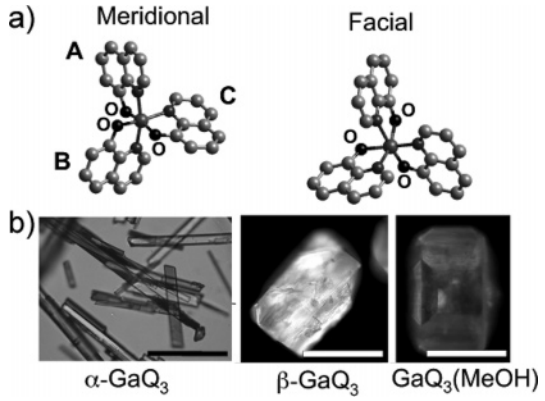

Figure 1. (a) Meridional (*mer*) and facial (*fac*) isomers of GaQ_3. The A, B, and C labels of the three quinoline ligands are identical to those used in the study of the vibrational modes of AlQ_3 by Esposti et al.[16] To illustrate the difference in molecular symmetry of the two isomers, we have labeled the oxygen atoms of the quinoline ligands. (b) Morphology of the various polymorphs of GaQ_3 observed by optical microscopy. The scale bar corresponds to 400 μm.

* Corresponding author. E-mail: Brinkman@ics.u-strasbg.fr.
† Institut Charles Sadron.
‡ Ecole de Chimie des Polymères et Matériaux.

(1) Hamada, Y. *IEEE Trans. Electron Devices* **1997**, *44*, 1206.
(2) Tang, C. W.; Van Slyke, S. A. *Appl. Phys. Lett.* **1987**, *51*, 913.
(3) Friend, R. H.; Gymer, R. W.; Holmes, A. B.; Burroughes, J. H.; Marks, R. N.; Taliani, C.; Dos Santos, D. A.; Brédas, J.-L.; Lögdlund, M.; Salaneck, W. R. *Nature (London)* **1999**, *397*, 121.
(4) Burrows, P. E.; Sapochak, L. S.; McCarty, D. M.; Forrest, S. R.; Thompson, M. E. *Appl. Phys. Lett.* **1994**, *64*, 2718.
(5) Brinkmann, M.; Gadret, G.; Muccini, M.; Taliani, C.; Masciocchi, N.; Sironi, A. *J. Am. Chem. Soc.* **2000**, *122*, 5147.
(6) Moulin, J.-F.; Brinkmann, M.; Thierry, T.; Wittmann, J.-C. *Adv. Mater.* **2002**, *14*, 436.

10.1021/cm049533n CCC: $27.50
Published on Web 07/10/2004

aged to produce blue-emitting AlQ_3 in the form of a new polymorph, δ, by simply annealing α-AlQ_3 powders under vacuum at approximately 410 °C.[8−10] It was demonstrated that the δ structure involves the facial isomer of AlQ_3 (see Figure 1).[10]

With the exception of AlQ_3 and InQ_3[11] the polymorphism of quinoline metal chelates has not been investigated thoroughly. Concerning GaQ_3, only one methanol clathrate has been identified by Wang et al.[12] Recently, Sapochak et al. reported that InQ_3 crystallizes in a structure which is isostructural to the β form of AlQ_3.[11] In the present study, we focus on the polymorphism of GaQ_3. Our aims are (i) to determine the crystal structures of the nonsolvated polymorphs of GaQ_3, (ii) to relate the structural characteristics to the fluorescence properties of the various polymorphs, and (iii) to understand the mechanism underlying the $\alpha \rightarrow \delta$ phase transformation induced by the annealing treatment proposed by Cölle et al. for AlQ_3.[9,10] Accordingly, the present work is organized into three parts. Section II reports the experimental conditions for the synthesis, the crystallization, and the structural and spectroscopic characterization of the samples. Section III contains the experimental results, and in section IV we discuss the mechanism for the $\alpha \rightarrow \delta$ phase transformation.

II. Experimental Section

GaQ_3 was synthesized by a simple reaction of the ligand hydroxyquinol in a 3:1 proportion with $GaCl_3$ in milliQ purified water. *Caution: $GaCl_3$ is highly reactive with water and generates HCl.* The formation of HCl was neutralized by an excess of potassium acetate. The solution was left under reflux for several hours at 40 °C which rapidly led to the formation of a yellow precipitate of GaQ_3. After completion of the reaction, the precipitate was filtered, washed with milliQ water, and dried under primary vacuum. The resulting material was purified twice by vacuum sublimation. Elemental analysis after sublimation for C, H, and N gave C = 64.42% (calc. 64.58), H = 3.57% (calc. 3.39) and N = 8.32% (calc. 8.97).

The α and β polymorphs were both obtained from recrystallization of a saturated solution in acetone in the dark and under inert atmosphere (N_2). We shall use in the following the same nomenclature of the polymorphs as reported for AlQ_3.[5,8] By a fast evaporation of acetone (50 mL/day), long needles with approximate size $400 \times 30 \times 30$ μm^3 of what is identified as the α polymorph were formed (see Figure 1b). In contrast, slow evaporation of acetone over several weeks (2−5 mL/day) leads to the formation of β-GaQ_3 with no traces of the α form as seen in Figure 2. The crystals of β-GaQ_3 grow as pseudo-hexagonal platelets (see Figure 1) with typical sizes of $500 \times 200 \times 50$ μm^3. Thus, the control of the crystallization kinetics enables preferential growth of the α or the β form of GaQ_3. In the case of the methanol clathrate, it was formed by crystallization of a saturated solution at −20 °C over a period of one week. This crystallization method leads to rhombohedral crystals of a methanol clathrate (see Figure 1). The δ polymorph of GaQ_3 was synthesized by the method described by Cölle et al. for AlQ_3.[9] A sample of pure α-GaQ_3 powder was sealed under high vacuum (10^{-5} mbar) in a Pyrex ampule. The sample was heated in an oven (Nabertherm) at a rate of 100 °C/h and left for 2 h at 380 °C before slowly cooling to room temperature. Some degradation of GaQ_3 was observed after annealing. The degradation which results in the presence of a small fraction of a brown residue is possibly due to the polycondensation of the quinoline ligand in the presence of water and/or O_2 traces.[13] δ-GaQ_3 crystallites are needle-shaped and very similar in shape and size to those of the α polymorph.

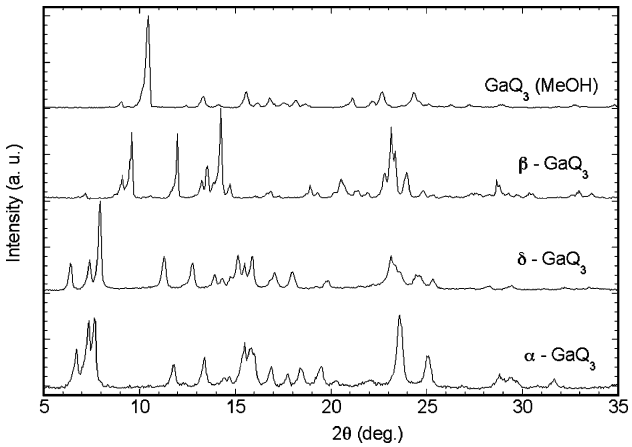

Figure 2. Experimental X-ray diffractograms of the various polymorphs of GaQ_3.

X-ray powder diffraction (XRPD) was performed with a Siemens D5000 diffractometer in (θ, 2θ) mode with a copper anode (Cu Kα, λ = 1.5418 Å) equipped with a graphite monochromator (2θ-scan range = 5−80°, scan step = 0.05° and 4 s/step). To obtain powder diffractograms with negligible preferential orientation, samples were gently ground in an agate mortar and the isotropic shape of the microcrystallites was subsequently checked with a Leica DMR-X microscope. Analysis of the X-ray diffractograms was performed with both TREOR and the Rietveld DBWS routines of the Cerius^2 program (Accelrys, Waltham MA, and Cambridge (UK)).[14] FT-IR spectra were recorded on the various polymorphs dispersed in KBr pellets using a Nicolet 210 spectrometer with a resolution of 1 cm^{-1}. Differential scanning calorimetry (DSC) was conducted by using a Perkin-Elmer DSC7 apparatus (heating rate of 20 °C/min) on α-GaQ_3 powders (5−10 mg) in aluminum cells.

Thin films were grown by high-vacuum sublimation (base pressure: 3×10^{-7} mbar) in a homemade evaporation system. The thickness and the deposition rate were measured by a quartz microbalance. The oriented films of PTFE were prepared as described in the literature.[6] For the TEM analysis, GaQ_3 was evaporated on PTFE supported by a carbon film onto copper grids. Electron diffraction and bright field imaging were performed on a Philipps CM12 transmission electron microscope equipped with a MegaView III CCD camera. Due to the high sensitivity of the CCD camera, the imaging was performed at very low electron irradiation levels.

III. Results

(A) Identification of the Polymorphs of GaQ_3. Figure 2 depicts the typical X-ray powder diffractograms of the various crystal structures of GaQ_3. These diffractograms are all clearly distinct from one another indicating that structurally pure polymorphs were obtained. The comparison between XRPD patterns of the GaQ_3

(7) (a) Brinkmann, M.; Biscarini, F.; Taliani, C.; Aiello, I.; Ghedini, M. *Phys. Rev. B* **2000**, *61*, 16339. (b) Brinkmann, M.; Graff, S.; Biscarini, F. *Phys. Rev. B* **2002**, *66*, 165430.

(8) Braun, M.; Gmeiner, J.; Tozlov, M.; Meyer, F. D.; Milius, W.; Hillebrecht, H.; Wendland, O.; von Schütz, J. U.; Brütting, W. *J. Chem. Phys.* **2001**, *114*, 9625.

(9) Cölle, M.; Gmeiner, J.; Milius, W.; Hillebrecht, H.; Brütting, W. *Adv. Funct. Mater.* **2003**, *13*, 108.

(10) Cölle, M.; Dinnebier, R. E.; Brütting, W. *Chem. Commun.* **2002**, 2908.

(11) Sapochak, L. S.; Ranasinghe, A.; Kohlmann, H.; Ferris, K. F.; Burrows, P. E. *Chem. Mater.* **2004**, *16* (3), 401−406.

(12) Wang, Y.; Zhang, W.; Li, Y.; Ye, L.; Yang, G. *Chem. Mater.* **1999**, *11*, 830.

(13) Papadimitrakopoulos, F.; Zhang, X.-M.; Thomsen, D. L.; Higginson, K. A. *Chem. Mater.* **1996**, *8*, 1363.

(14) Cerius^2 User's Guide section on *Computational Instruments, Diffraction and Microscopy*; p 131 and references therein.

Table 1. Unit Cell Parameters Gained from the Rietveld Refinement of PXRD Data of GaQ_3

polymorph	α	β	δ	$GaQ_3(CH_3OH)$
type	triclinic	triclinic	triclinic	monoclinic
space group	$P\bar{1}$	$P\bar{1}$	$P\bar{1}$	$P2_1/n$
a (Å)	6.27	8.4	6.2	11.0
b (Å)	13.0	10.30	13.30	13.2
c (Å)	14.8	13.2	14.55	16.9
α (deg)	110.0	108.6	114.2	
β (deg)	89.2	97.3	88.4	97.2
γ (deg)	98.0	89.9	96.1	
Z	2	2	2	4
V (Å^3)	1123	1078	1081	2434
R_P (%)	10.9	15.64	12.3	12.7
R_{WP} (%)	14.4	20.2	15.2	15.9

polymorphs and the AlQ_3 analogues prepared in the same experimental conditions[5,9] reveals their isostructural character. This isomorphism of tris(8-hydroxyquinoline)M(III) chelates is further supported by a recent study by Sapochak et al.[11] on InQ_3 which is found to crystallize in a structure which is isostructural to the β form of AlQ_3. A similar and well-known structural isomorphism is observed in the case of metal phthalocyanines[15] for a large variety of metals M(II) (M = Cu, Ni, Zn, ...).

The samples of α and β polymorphs are crystallographically pure since the corresponding diffractograms reproduce all the expected diffraction peaks reported for the AlQ_3 analogue. It is worth mentioning that the difference in crystallization conditions between α and β forms was not recognized in earlier studies on AlQ_3.[5] Figure 2 clearly shows that the thermal treatment of α-GaQ_3 at 380 °C fully converts the α structure into a different polymorph identified as δ by comparison with the Al(III) analogue.

The possibility to control and prepare crystallographically "pure" phases of GaQ_3 allowed us to determine the unit cell parameters of the various GaQ_3 polymorphs. A first trial set of unit cell parameters was determined by using successively the TREOR and the DWBS Rietveld refinement routines. For the input structures in the DWBS method, we used the structures of the aluminum analogues and simply replaced Al with Ga in the atomic coordinate files, i.e., we maintained the fractional coordinates of all atoms in the unit cell. In Figure 2, we present the best result obtained in the case of the α polymorph which leads to $R_P = 10.02\%$ and $R_{WP} = 14.3\%$. The low values of R_P and R_{WP} are very similar to those in ref 5 and demonstrate that GaQ_3 and AlQ_3 are isomorphous with respect to the α polymorph. This implies that, not only do the α polymorphs of AlQ_3 and GaQ_3 share similar unit cells (see Table 1), but, they both imply a racemic mixture of both enantiomers of the *mer* isomer.

Concerning the β polymorph, the Rietveld refinement gave slightly higher R_P and R_{WP} values of 15.6% and 20.2%, respectively. This suggests that atomic fractional coordinates are slightly different for the β polymorph of GaQ_3 with respect to AlQ_3. However, the rather good agreement between experimental PXRD and the refined plot suggests that *mer*-GaQ_3 is present in this polymorph. This will also be demonstrated by FT-IR in the subsequent section. Concerning the δ polymorph, it has been obtained by annealing at 380 °C under vacuum either the α or the β polymorphs of *mer*-GaQ_3. The typical PXRD is shown in Figure 2 which is very similar to that reported by Cölle et al. for δ-AlQ_3. The unit cell parameters obtained from TREOR are listed in Table 1. Notice that α and δ polymorphs of AlQ_3 show almost the same reduced unit cell parameters and the same space group. These two polymorphs differ mainly in the isomer, namely *mer* and *fac* for the α and δ polymorphs, respectively.[8−10] As a consequence, the diffractograms of the α and δ structures look rather similar (see Figure 2). This prompted us to use as starting structures for the Rieveld refinement procedure of δ-GaQ_3 both the α and δ structures of AlQ_3 after substitution of Al for Ga. The best results of the Rietveld refinement are obtained for the δ structure which yields $R_P = 12.7\%$ and $R_{WP} = 15.9\%$, whereas by using the α structure as starting point we obtain $R_P = 17.3\%$ and $R_{WP} = 21.2\%$. This result suggests that δ-GaQ_3 contains mainly the facial isomer similarly to δ-AlQ_3. Further proof of the presence of the facial isomer will be given by FT-IR spectroscopy (vide infra).

A methanol clathrate has also been produced by crystallization at −20 °C of a saturated GaQ_3 solution in methanol. The PXRD in Figure 1 is as expected for the clathrate structure as reported in ref 12 with the composition $GaQ_3(CH_3OH)$. This clathrate of GaQ_3 is also a racemate of the *mer* isomer and crystallizes in a monoclinic structure (see Table 1).[5,12]

In summary, we have demonstrated that the crystal structures of AlQ_3 and GaQ_3 are isomorphous and involve either the *mer* (α and β polymorphs and clathrates) or the *fac* isomer (δ structure).

(B) Spectroscopic Identification of Facial and Meridional Isomers of GaQ_3. To ascertain the previous assumptions concerning the isomers present in the different polymorphs of GaQ_3, FT-IR spectra of the different samples were collected and are plotted in Figure 4. Qualitatively, the α and β polymorphs exhibit rather similar spectra. The β structure shows the sharpest peaks (see for instance the structured peaks around 800 cm^{-1}). This entails the higher degree of crystallinity of the β structure with respect to the α structure as evidenced by XRPD. The FT-IR spectrum of the δ form exhibits remarkable differences from those of α and β. We will analyze these differences using the nomenclature of the vibrational modes established by Esposti et al. for the infrared and Raman spectra of *mer*-AlQ_3.[16]

First, we note strong similarites in the FT-IR peak intensities and positions for β-GaQ_3 and β-AlQ_3 in the range 750−1600 cm^{-1} which contains mainly vibrational modes of the quinolinate ligands. In the range 400−750 cm^{-1} significant differences are observed which traduce the effect of the substitution of Al by Ga. For instance, the modes involving the Ga···O bond ν_{GaO}^x (x = A,B,C ligands) are all shifted toward lower energies by approximately 25−27 cm^{-1} (see Figure 4) and appear around 520 cm^{-1}.

To identify the isomers involved in the β and δ structures, we shall first determine the modes that can be ascribed to A, B, and C ligands for the *mer* isomer with C_1 symmetry. This task is rather difficult since

(15) Leznoff, C. C.; Lever, A. B. P. In *Phthalocyanines*; VCH: Weinheim, 1989; vol. I, p. 397.

(16) (a) Esposti, A. D.; Brinkmann, M.; Ruani, G. *J. Chem. Phys.* **2002**, *116*, 798. (b) Esposti, A. D.; Brinkmann, M.; Ruani, G.; Zamboni, R. *Synth. Met.* **2002**, *127*, 247

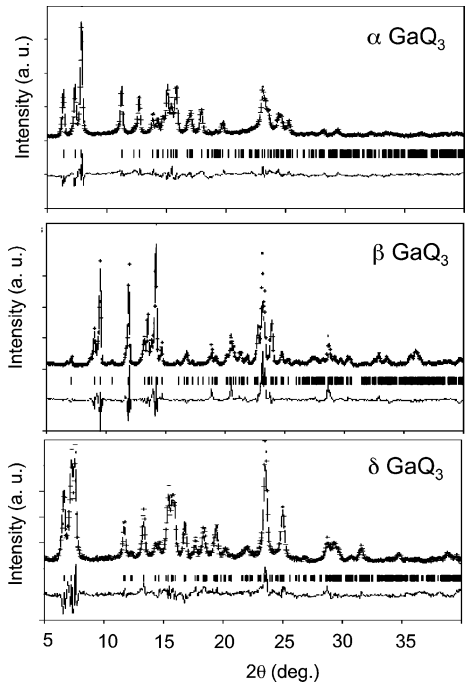

Figure 3. Rietveld refinement plots of the PXRD data of Figure 2 for the α, *β*, and *δ* polymorphs of GaQ_3. All figures show the experimental data (+), the Rietveld refinement plot (continuous line), and the difference spectrum.

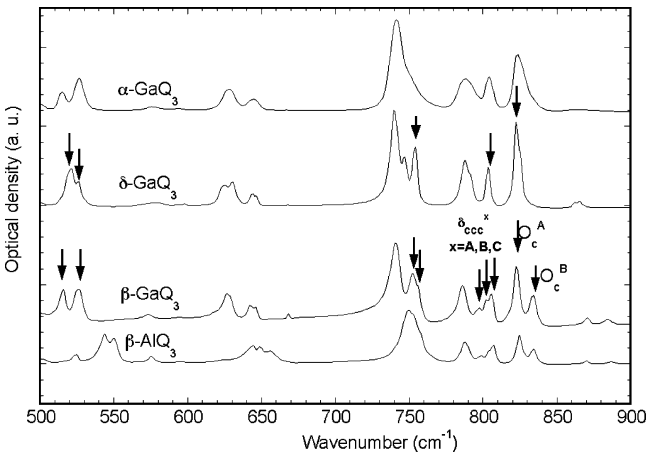

Figure 4. FT-IR spectra of α, *β*, and *δ* polymorphs. Mode assignments have been made according to ref 16 for the *mer* isomer (see text).

most vibrational modes of the A, B, and C ligands in *mer*-AlQ_3 are found to be coupled to one another and only a few modes are clear signatures of single quinolinate fragments.[16]

The work by Esposti et al. demonstrated that the pyramidalization modes O_{CCC} are clearly distinct for all three (A, B, and C) quinolinate fragments in the *mer* isomer and give rise to three distinct peaks with calculated positions at 820.2, 824.3, and 826.2 cm^{-1} and similar intensities for the A, C, and B ligands, respectively.[16] The modes observed for *β*-AlQ_3 and *β*-GaQ_3 (see Figure 3) at 824 and 834 cm^{-1} can be attributed to the pyramidalization modes O_c^A and O_c^C of the A and C ligands, respectively. In contrast, given the C_3 symmetry of the *fac* isomer, which is assumed to be present in the *δ* polymorph, only one rather narrow peak at approximately 824 cm^{-1} with a small shoulder is observed for *δ*-GaQ_3 (see Figure 4). The same type of

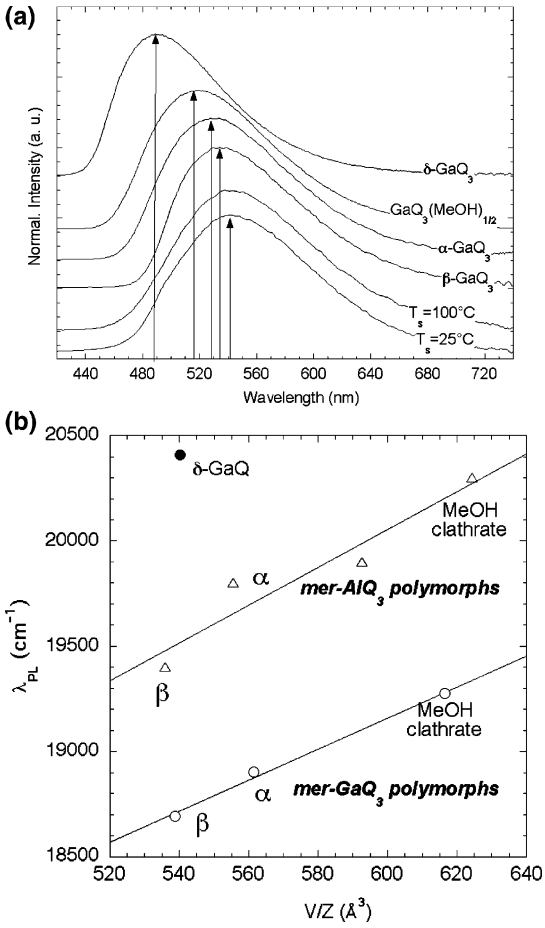

Figure 5. (a) Comparison of the fluorescence spectra at 293 K of the various polymorphs of GaQ_3 with amorphous and crystalline thin films grown onto oriented PTFE. For clarity, all PL intensities have been normalized to unity and successive spectra were shifted along the ordinate axis. (b) Correlation between the maximum of fluorescence λ_{max} at 293 K and the molecular volume *V/Z* in the various polymorphs of GaQ_3 involving the *mer* isomer. The data concerning AlQ_3 are taken from ref 5.

observation can be made in the case of the peaks around 750 cm^{-1} which can also be attributed to pyramidalization modes of the type O_C^x (x = A, B, C).[16]

In a similar manner, the angle bending modes of the type δ_{CCC} allow us to differentiate the *fac* and *mer* isomers. From the calculations of ref 16, A, B, and C ligands in *mer*-AlQ_3 are expected to give rise to three δ_{CCC} bands at 793.2, 792.4, and 791.7 cm^{-1}. The 807 and 804 cm^{-1} peaks were accordingly attributed to $\delta_{CCC}{}^C$ and $\delta_{CCC}{}^B$ modes, respectively. Since the FT-IR spectra of GaQ_3 and AlQ_3 are almost identical around 800 cm^{-1}, the same assignment can be done for *mer*-GaQ_3 in the *β* structure. As seen in Figure 4, only one single and narrow line is observed at 804 cm^{-1} in *δ*-GaQ_3, suggesting a different molecular symmetry of GaQ_3.

To summarize, the two vibrational modes δ_{CCC} and O_{CCC} are typical fingerprints that allow distinction of *mer* and *fac* isomers. Only the α and *β* polymorphs exhibit typical bands which are characteristic of the A, B, and C quinolinate fragments because of the low molecular symmetry C_1. The absence of similar splittings of the δ_{CCC} and O_{CCC} modes in the *δ* structure ascertains the presence of the facial isomer in this crystal structure.

(C) Fluorescence. In Figure 5a, we depict the fluorescence spectra at 293 K of the various GaQ_3 polymorphs as well as amorphous and crystalline films of the α form. At first glance, the maximum of emission λ_{max} shows a clear dependence on the structure. λ_{max} is observed to vary in a large range between 542 nm (18 450 cm^{-1}) in amorphous thin films and 489 nm (20 450 cm^{-1}) for the blue-emitting δ-GaQ_3. In Figure 5b, we have plotted the maximum of fluorescence λ_{max} as a function of the volume per molecule *V/Z* for AlQ_3 and GaQ_3 which quantifies the compacity of the molecular packing in the various crystal structures. The same tendency is observed for all structures involving the *mer* isomer of GaQ_3 and AlQ_3: λ_{max} scales almost linearly with *V/Z*. Interestingly, the case of the δ polymorph of AlQ_3 and GaQ_3 does not follow the same trend. α and δ polymorphs have almost the same crystal densities (see Table 1) but exhibit very different fluorescence maxima at 528 nm (18 940 cm^{-1}) and 489 nm (20 450 cm^{-1}), respectively. This indicates that the blue shift of fluorescence in the δ structures of GaQ_3 and AlQ_3 has a molecular origin. This result is in agreement with the recent calculations by Amati and Lelj who predicted a blue-shift of approximately 23 nm of the emission of the *fac* isomer with respect to the *mer* isomer.[17]

For all polymorphs of *mer*-GaQ_3, the emission maximum λ_{max} is found to be red-shifted by approximately 750 cm^{-1} with respect to AlQ_3 (see Figure 5). Similarly to the case of AlQ_3, the most red-shifted emission is observed for amorphous thin films. The strong red-shifted emission in amorphous films might be explained in terms of a denser packing of the molecules in the amorphous state with respect to the crystalline polymorphs. By extrapolating the linear curve in Figure 5, we see that a small variation of the volume per molecule of 3−4% is sufficient to explain the observed value of λ_{max}. A denser packing of the amorphous phase would explain the peculiar stability of amorphous thin films used in OLEDs against crystallization. It is rather surprising that the crystalline films grown at $T_s = 100$ °C (α structure) do not exhibit a more blue-shifted fluorescence as observed for α powders. As shown in the following, this can be attributed to the high degree of disorder observed in the α microcrystallites as evidenced by TEM (vide infra).

(D) Crystalline Films of α GaQ_3. As demonstrated by Moulin et al., the crystallization of AlQ_3 can be achieved onto oriented PTFE substrates at a substrate temperature $T_s = 100$ °C. We therefore verified that the same deposition conditions (deposition rate and substrate temperature) would also result in crystalline films of α-GaQ_3. As seen in Figure 6, GaQ_3 films grown in these deposition conditions are polycrystalline. The needles show typical sizes of 1−2 μm length and 50−100 nm width. The needles of GaQ_3 show the same orientations as observed in the case of AlQ_3, namely parallel and at ±60° with respect to the chain axis of PTFE $\mathbf{c_{PTFE}}$.[6] The coexistence of three crystal orientations is also visible in the diffraction pattern in Figure 6b. The selected area electron diffraction (SAED) pattern in Figure 6c has been indexed by using the unit cell of the α structure. The most intense reflexes are identified as (1 0 1) and (1 1 −3) (see Figure 6). The needle axis is identified as the **a** axis and the contact plane on the PTFE substrate corresponds to the (**a**,**c**) plane (Figure 7). A look to the α structure of GaQ_3 shows that the **a** axis coincides with the distance of closest packing of GaQ_3 molecules.

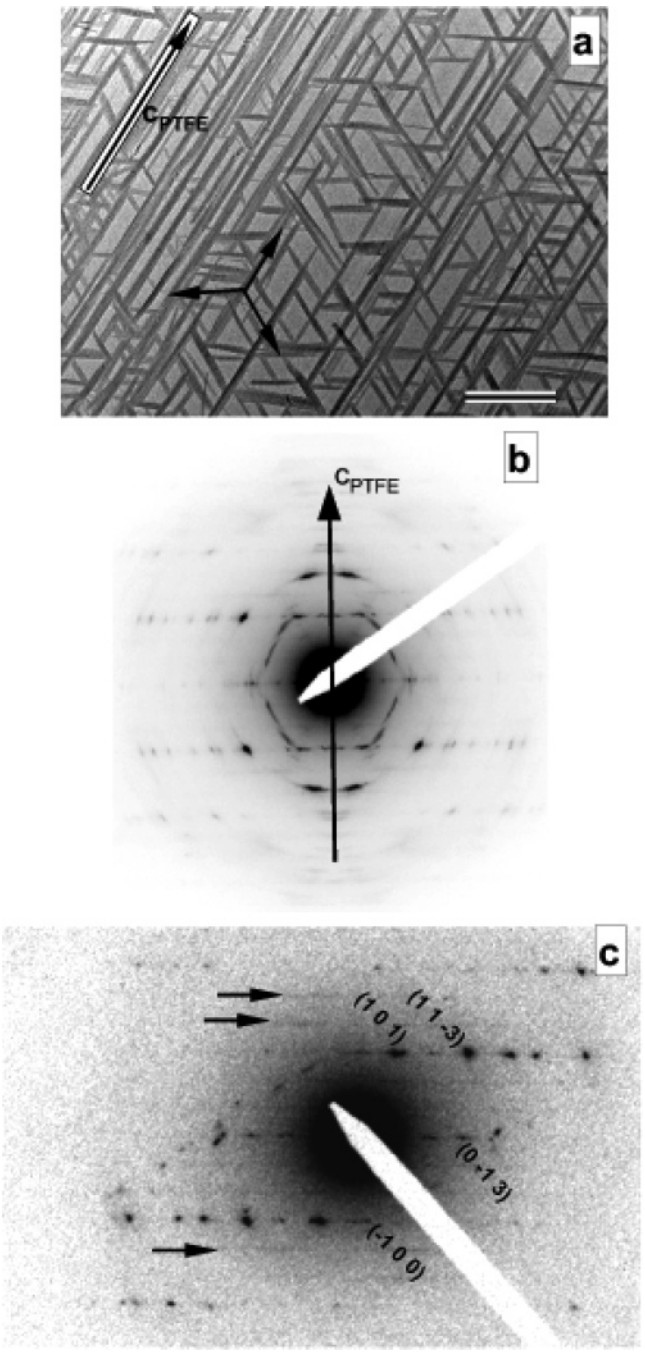

Figure 6. Morphology in vacuum-deposited thin films of GaQ_3 (50 nm) onto oriented PTFE for $T_s = 373$ K. (a) Bright field micrograph. The scale bar corresponds to 1 μm. (b) Diffraction pattern, the chain axis of PTFE corresponds to $\mathbf{c_{PTFE}}$ and is indicated by an arrow. (c) Selected area electron diffraction pattern of one α-GaQ_3 needle. The most intense reflections have been indexed using the reduced unit cell of α-GaQ_3. Arrows point at streaks which are due to structural disorder (see text).

The SAED pattern in Figure 6c shows also very characteristic streaks indicated by arrows which appear at one-third of the (1 0 0) periodicity. Presence of this kind of streaks is a typical fingerprint of twinning which

(17) (a) Amati, M.; Lelj, L. *Chem. Phys. Lett.* **2002**, 358, 144. (b) Amati, M.; Lelj, F. *J. Phys. Chem. A* **2003**, *107*, 2560.

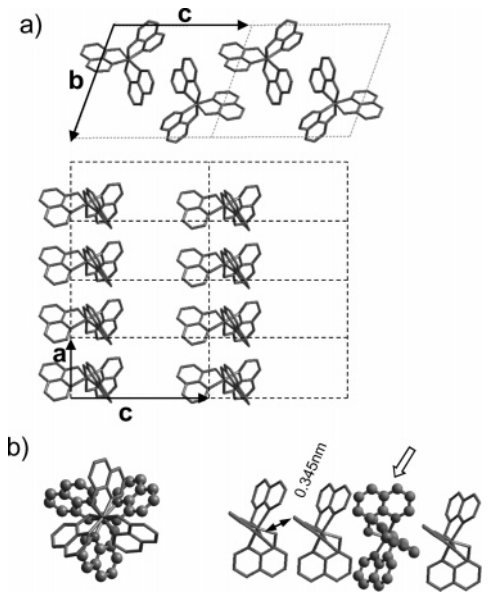

Figure 7. (a) Section view and top view of the (**a**,**c**) contact plane of GaQ_3 onto oriented PTFE substrate. (b) Typical defect in an **a**-stack of GaQ_3 molecules obtained by the substitution of one enantiomer which has been drawn in stick and ball. Also shown is the shortest inter-ligand distance of 0.345 nm along the stacking axis.

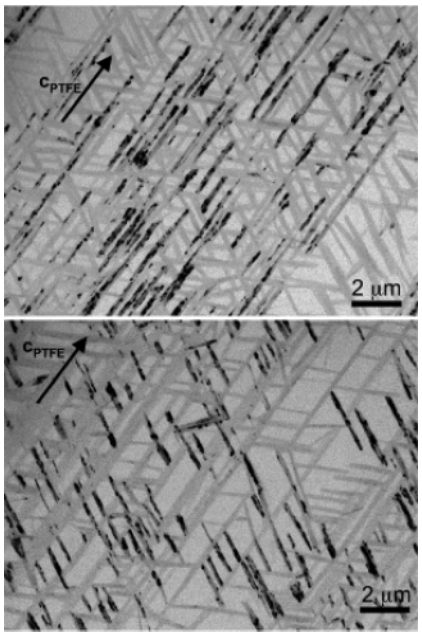

Figure 8. Dark field images obtained from the (1 1 −3) reflection of α-GaQ_3 domains oriented parallel and at 60° from the $\mathbf{c_{PTFE}}$ axis.

is frequently observed in molecular crystals such as C_6Br_6 and phthalocyanines.[18,19] The precise determination of the twinning axis is presently in progress and will be reported elsewhere. Further evidence for structural defects within GaQ_3 needles is obtained by using the dark field imaging technique. Figure 8 depicts the dark field images obtained by selecting one of the brightest reflexes, i.e., (1 1 −3) successively for the orientation parallel to $\mathbf{c_{PTFE}}$ and at 60°. Interestingly, we observe that only parts of the needles appear dark in the TEM micrographs of Figure 8. The domains corresponding to dark areas are of elongated shape along the **a** axis (needle axis) and distributed at random within the needles. This result is similar to that observed in the case of sexiphenyl needles on mica substrate[20] and suggests that the needles have a polycrystalline nature, i.e., consist of microdomains with different crystallographic orientations.

Stacking faults between columns of strongly interacting molecules are well-known to occur in phthalocyanines. Such defects appear mainly because of the anisotropy of intermolecular interactions in the crystal.[18] We have calculated the van der Waals (VdW) interactions between the nearest neighbor molecules $E_{Mol-Mol}$ along the various crystallographic axes of α-GaQ_3.We observe that $E_{Mol-Mol}$ depends significantly on the crystallographic direction in the crystal. For instance, the calculated VdW interaction $E_{Mol-Mol}$ along the **a** axis amounts to 11.7 kcal/mol vs 1.11 kcal/mol and 0.2 kcal/mol along the **b** and **c** axes, respectively. It appears therefore natural to observe disorder along the **c** axis between successive **a**-stacks. In addition to the typical stacking faults observed in phthalocyanines for instance, the racemic character of the α structure is likely to induce a new type of defects. Indeed, we see that the molecular stacks along the **a** axis involve exclusively one of the two enantiomers of the *mer* isomer. However, it is envisagable to mix both enantiomers within a given **a**-stack without too much perturbing the intermolecular distance within the stacks. This is shown in Figure 7b where one enantiomer of GaQ_3 has been replaced by the other without inducing additional steric hindrance. This type of defect seems all the more likely to occur as the growth kinetics is fast and far from equilibrium conditions.

IV. Discussion

As demonstrated by Curioni et al.[21] the *mer* isomer is more stable by 4.0 kcal/mol with respect to the *fac*-AlQ_3. The *mer*→*fac* isomerization is thus expected to be endothermic. In contrast to this, DSC measurements indicate that the α→δ transformation is exothermic (approximately 0.96 kcal/mol) indicating that the cost of the isomerization reaction is counterbalanced by the gain in the crystal packing energy.

The unit cell parameters found for α and δ structures are very similar and the relative variation does not exceed 4%. This means the α and δ polymorphs differ mainly in the isomer, *mer* in the α form and *fac* in the δ form (see Figure 9). As shown in Figure 9, the change of the *mer* isomer by thermal annealing involves a specific ligand labeled C (respectively C′ for the symmetry-related molecule). Comparing the α and δ structures (see Figure 9), we see that the *mer*→*fac* isomerization requires a 180° ligand flip of the C ligand around the bisector of the bond angle N···Ga···O. A close look

(18) Kobayashi, T. In *Crystals: Growth, Properties and Applications*; Springer-Verlag: Berlin/Heidelberg, 1991; p 41.

(19) Kitaigorodsky, A. I. In *Molecular Crystals and Molecules*; Academic Press: New York, 1973.

(20) Plank, H.; Resel, R.; Sitter, H.; Andreev, A.; Sariciftci, N. S.; Hlawacek, G.; Teichert, C.; Thierry, A.; Lotz, B. *Thin Solid Films* **2003**, *443*, 108.

(21) Curioni, A.; Boreo, M.; Andreoni, W. *Chem. Phys. Lett.* **1998**, *294*, 263.

(22) Destro, R.; Gavezotti, A. In *Structure and Properties of Molecular Crystals*; Pierrot, M., Ed.; Elsevier: Amsterdam, 1990; p 200.

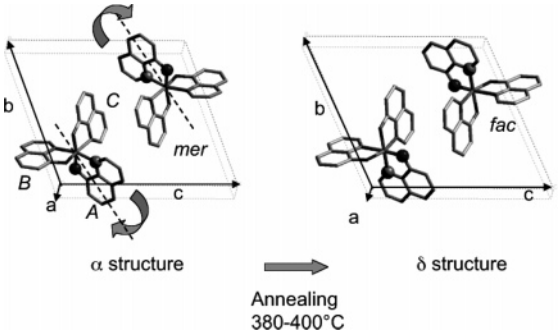

Figure 9. Comparison of the unit cells for α and δ polymorphs of GaQ_3. The structural α→δ transformation can be described as a *mer*→*fac* isomerization in the solid-state involving a ligand flip when the α structure is annealed at 380 °C. The oxygen and nitrogen atoms that are exchanged with another are drawn as spheres.

at the crystal structure shows that the ligand flip cannot occur without steric hindrance in the crystal structure at room temperature. However, at the transition temperature (380−400 °C), the dilation of the unit cell as well as the molecular motions of large amplitude within the crystal[22] open the possibility to overcome the steric hindrance associated with the ligand flip. Given the rather short contacts between the C ligands along the **a** axis (0.345 nm), it is very likely that ligand flips occur in a collective manner.

V. Conclusions

The present study has uncovered the structural isomorphism of GaQ_3 with the aluminum analogue AlQ_3 concerning both the nonsolvated α, β, and δ structures and the clathrates. XRPD and FT-IR spectroscopy demonstrate that the α, β, and the clathrates contain the *mer* isomer of GaQ_3 whereas the *fac* isomer is present in the only δ structure obtained after annealing of the α structure under vacuum at 380 °C. This result suggests that, similarly to metal phthalocyanines, MQ_3 metal chelates (M = Al, Ga, In, etc...) show a typical isomorphism. This observation opens several perspectives of interest such as the possibility to grow mixed crystals by epitaxial crystallization of different metal chelates having different properties, e.g., magnetic in the case of FeQ_3 and CoQ_3 and electroluminescent for GaQ_3 and AlQ_3. Similarly to AlQ_3, the maximum of fluorescence of *mer* GaQ_3 is clearly correlated to the crystal density in the α, β structures and the clathrates. The comparative study of the α and δ structures allows us to draw a scheme for the phase transformation of GaQ_3 and AlQ_3 by thermal annealing. The structural α→δ transformation can be described as a solid-state isomerization reaction of the type *mer*→*fac* which does not substantially alter the crystal structure of the intial α structure. In thin films, we have demonstrated the possibility to grow the α structure onto oriented PTFE substrate. In addition, electron diffraction and dark field imaging reveal the presence of important structural defects caused by both the high anisotropy of intermolecular interactions in the α structure of GaQ_3 and the racemic character of the evaported material.

Acknowledgment. Frank Nüesch and Libero Zuppiroli are gratefully acknowledged for giving us access to the fluorescence facility at EPFL. Jacques Druz and Richard Nuffer are acknowledged for technical support. We also acknowledge Bernard Lotz and Frédéric Péruch for stimulating discussions.

CM049533N